

Above-Threshold Ionization in Low-Frequency Limit

T. F. Gallagher

Department of Physics, University of Virginia, Charlottesville, Virginia 22901

(Received 15 August 1988)

Above-threshold ionization of Rydberg atoms by microwave intensities of 3×10^4 W/cm² produces electrons with kinetic energies of up to 9 eV, corresponding to the absorption of up to 3×10^5 photons. The observations can be described in terms of a classical free electron in an oscillating field, which is the low-frequency limit of more conventional treatments of the phenomenon.

PACS numbers: 32.80. RM

One of the more interesting effects observed in the multiphoton ionization of atoms by intense laser fields is above-threshold ionization (ATI), the absorption by the atom of more photons than the minimum number required to reach the ionization limit. This phenomenon, first observed by Agostini *et al.*¹ is manifested in the energy spectrum of the ejected photoelectrons as a series of peaks separated in energy by the photon energy, not simply one peak corresponding to the absorption of the minimum number of photons. Somewhat later, Kruit *et al.* observed that the lowest-energy peaks disappear as the laser intensity is increased.² This phenomenon was attributed to the increase of the ionization limit by the ponderomotive potential $W_p = e^2 E^2 / 4m\omega^2$, which is the average oscillation energy of a free electron of charge e and mass m in an oscillating electric field $E \sin \omega t$.³

When the ejected electron leaves the laser field, spatially defined by the focus of the laser beam, the oscillation energy, W_p , is converted into directed translational motion so that the energies of the ejected electrons are independent of the ponderomotive shift of the limit. The equivalence of the electron's leaving the focus of the field to leaving a region of potential energy W_p has been demonstrated very elegantly by Bucksbaum, Bashkansky, and McIlrath,⁴ who explicitly observed the scattering of free electrons by an optical ponderomotive potential.

Theoretically, ATI is usually treated by consideration of a free electron in an electromagnetic field, ignoring the Coulomb potential of the atom.^{5,6} In such treatments the ponderomotive potential sets the approximate scale of the ATI which is observed. Unfortunately, the intimate connection between ATI and W_p is not particularly transparent in most treatments, but as we shall see, in the low-frequency limit the connection is clear.

Here we report the first investigation of ATI in the low-frequency limit, specifically of Na Rydberg atoms by an 8.2-GHz microwave field. This frequency is a factor of 3×10^4 smaller than that of a Nd-doped yttrium-aluminum-garnet (Nd:YAIG) laser, and in principle, the same ponderomotive potential should be produced by an intensity 10^9 times smaller, i.e. a 1-eV ponderomotive potential should be produced by an 8.2-GHz intensity of

10^4 W/cm², as opposed to 10^{13} W/cm² of a Nd:YAIG laser light. Although it is not *a priori* obvious that the same physical situation obtains over such a range of parameters, we shall see that experimental results are fitted by a model based on a classical description of a free electron in an oscillating field, which is the classical low-frequency limit of quantum-mechanical treatments.^{5,6}

The general idea of the experiment is to excite Na Rydberg atoms to a point near the zero-field ionization limit in the presence of a 8.2-GHz microwave field and examine the kinetic energies of the ejected electrons with an energy analyzer. The apparatus, save the analyzer, has been described previously,⁷ so its description here is brief. A horizontally directed thermal Na beam enters a microwave cavity through a 1-mm-diam hole in one sidewall, and two counterpropagating pulsed dye-laser beams enter the cavity through a similar hole in the opposite sidewall. The lasers are tuned to the Na $3s \rightarrow 3p$ and $3p \rightarrow ns$ transitions to excite the Na atoms to a Rydberg state. There is a 1-mm-diam hole in the center of the top of the cavity through which electrons liberated below the hole can escape to the detector. The cavity operates on the TE₁₀₁ mode with its electric field vertical, and only electrons from the electric-field antinode are observed at the detector. The cavity has a copper septum which permits field ionization of the excited atoms but does not affect the microwave field. The cavity has a resonant frequency of 8.20 GHz and a Q of 925. The microwave source is a Hewlett Packard model 8350B/83550A sweep oscillator plug-in, which is attenuated with a precision Hewlett Packard model X382A attenuator and amplified by a Litton 624 traveling-wave tube amplifier, which is gated on for 1 μ s at each pulse of the laser. After the amplifier, the microwave power passes to the cavity through a 20-dB coupler, which allows the power to be monitored by a Hewlett Packard model 432 power meter, and a circulator, which allows the reflected microwave power to be monitored. To monitor drifts in the microwave power level, the microwave ionization threshold field of the Na $23s$ state is measured periodically with the method described previously.⁷ The uncertainty in the microwave power measurements is 15%.

To observe individual ATI electron peaks, which are $< 10^{-4}$ eV apart, is hopeless. Our goal is to examine their envelope, and to this end we have used a simple retarding-field electron spectrometer. There is a grounded plate 3 cm above the microwave cavity with a 6-mm-diam hole covered by a fine copper mesh, defining an acceptance angle of ~ 0.12 sr. Above the plate is the retarding potential grid, to which a variable potential is applied, and the dual microchannel-plate detector. The whole assembly is enclosed by a 0.25-mm-thick CoNetic magnetic shield which reduces the magnetic field to < 50 mG. With this arrangement we have an energy resolution of $\frac{1}{2}$ eV.

The 5-ns laser pulses arrive in the center of the 1- μ s microwave pulse, and the electrons are detected by a gated integrator with a 100-ns gate. For a given microwave power, the electron signal is recorded while we repetitively sweep the voltage on the retarding potential grid and store the accumulated results in a computer. Figure 1 shows the retarding potential scans with the second laser set to the wavelength of the 15s state, bound by 590 cm^{-1} , and the 40s state, bound by 73 cm^{-1} . For simpli-

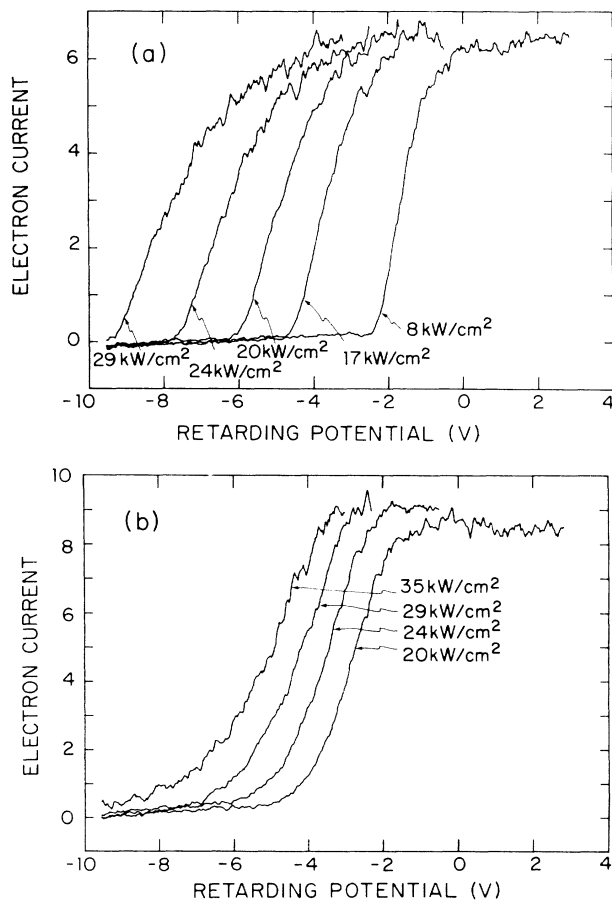


FIG. 1. Retarding-field scans for (a) the 40s state and (b) the 15s state at several microwave intensities, from 8 to 35 kW/cm^2 .

city, we shall refer to these data as the 15s and 40s data, remembering that s states are no longer good quantum states in the microwave field. From these data it is immediately apparent that electrons are ejected with as much as 9 eV of energy, which corresponds to the absorption of $\sim 3 \times 10^5$ microwave photons, and that the energy of the ejected electrons increases with microwave intensity. In addition, the magnitude of the observed ATI signals is approximately an order of magnitude smaller than the spatially integrated electron signals obtained by field ionization, implying a strongly peaked angular distribution. The derivatives of the retarding-potential scans shown in Fig. 1 yield the electron energy distributions. In Fig. 2 we show the 15s and 40s electron energy spectra for the same microwave intensity of 24 kW/cm^2 . The 40s electron energy spectrum has a sharp high-energy edge, falling gradually at lower energies, and the reverse is true for the 15s spectrum, which has a sharp low-energy edge and falls gradually at higher energies. The spectra for 30s and $n \rightarrow \infty$ resemble the 40s spectrum, and the 20s spectrum is more similar to the 15s spectrum.

At powers where microwave ionization occurs, there is only a smooth dependence on the wavelength of the second laser. Resonances due to ponderomotive energy shifts of high-lying levels, as observed by Freeman *et al.*,⁸ are conspicuously absent, in spite of the fact that the ponderomotive shifts of the levels excited by the second laser range from negligibly small for the lowest levels to quite large, ~ 1 eV, as $n \rightarrow \infty$. Any such shifts are masked by the effectively continuous spectrum of unresolved sideband states 8.2 GHz apart, which originate from the large first-order Stark shifts in the microwave field.⁹ We also note that changing the laser intensities only alters the magnitude of the electron signal but not the energy distribution of the ejected electrons.

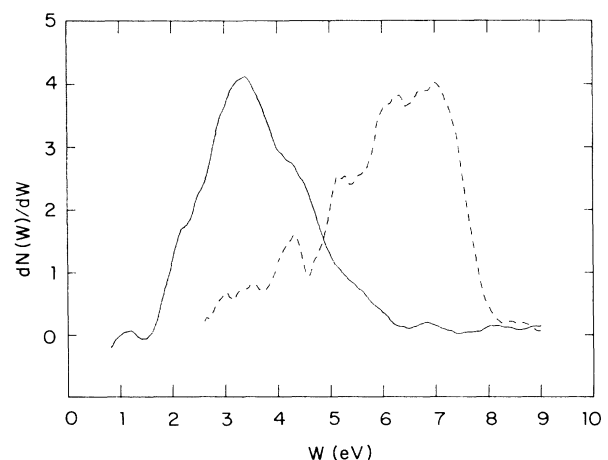


FIG. 2. Electron energy distributions for the 40s state (---) and the 15s state (—) at an intensity of 24 kW/cm^2 for which $W_p = 1.6$ eV.

The above observations can be compared to a simple classical model which is nearly identical to one previously given by van Linden van den Heuvell and Muller.¹⁰ If an electron is created at rest at time t_0 in an electric field $E \sin \omega t$, it has at a later time t with velocity

$$v \equiv \frac{eE}{m\omega} (\cos \omega t - \cos \omega t_0). \quad (1)$$

In the microwave field, it therefore has the average kinetic energy of

$$\langle \frac{1}{2} m v^2 \rangle = \frac{e^2 E^2}{4m\omega^2} (1 + 2 \cos^2 \omega t_0), \quad (2)$$

where the first term in the parentheses is the energy of the oscillatory motion and the second is the energy of the directed translational motion. Since the oscillatory energy is converted to directed energy when the electron leaves the field, Eq. (2) describes the expected electron energy spectrum. From Eq. (2) it is apparent that the electron energy spectrum lies between W_p and $3W_p$; however, the details depend upon t_0 , the instant the electron is created in the field. The sensitivity to t_0 , or equivalently to the microwave phase, is similar to a result of Kroll and Watson.¹¹ In practice, t_0 is the time of ionization, when the electron becomes free of the atom. Note that the free-electron model, which describes the electron energy spectrum, does not tell us how or when the electron becomes free of the atom. Free-electron models, in general, are flawed in such respects.¹² To determine t_0 , we recall first that the laser pulses are 5 ns long, covering 40 microwave cycles. For a continuum state, or high-lying state, which is field ionized by a field much less than the maximum of the microwave field, t_0 can be very nearly any time in the microwave cycle. For a low-lying state, which is hard to ionize, the electron only becomes free at the peak of the microwave field, $\omega t_0 \sim \pi/2$. The number of electrons $dN(W)$ observed in the small energy range dW around $W_p(1 + 2 \cos^2 \omega t_0)$ is determined by the probability that ionization occurs in the corresponding time interval dt_0 around t_0 . This is shown graphically in Fig. 3 for two cases; high n , > 30 , for which all values of t_0 are allowed, and low n , ~ 15 , for which $\pi/4 < \omega t_0 < \pi/2$. In other words, we have some control over the phase of the microwave field at which the electron becomes free.

There is an obvious qualitative difference between the experimental 40s spectrum of Fig. 2 and the theoretical high- n spectrum of Fig. 3; the low-energy peak is suppressed. The suppression is due to a geometric lens effect which occurs as the electrons leave the cavity and is related to one observed by Freeman *et al.*¹³ All the electrons gain a translational kinetic energy of W_p when they leave the microwave field. For the lowest-energy electrons detected, this is the largest part of their energy. While all the electrons gain the same amount of translational energy, they are accelerated in different directions by the ponderomotive force $\vec{F}_p = -(e^2/4m\omega^2)\nabla E^2$. If

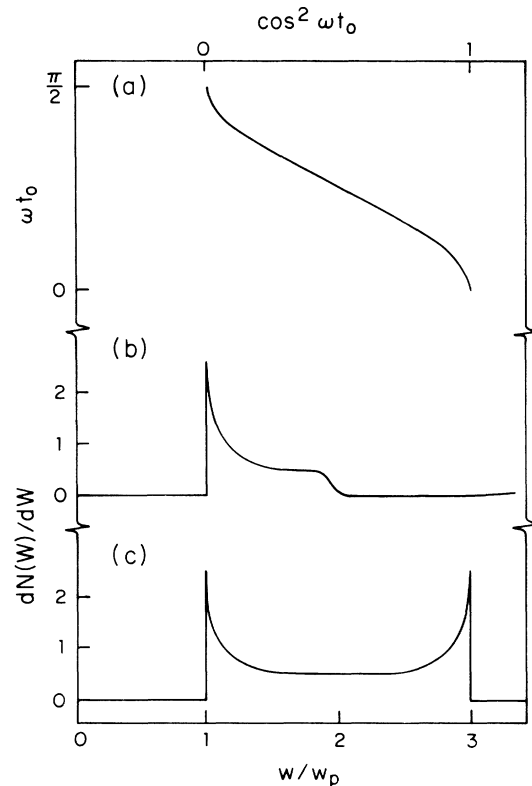


FIG. 3. A plot of (a) $\cos^2 \omega t_0$ showing how it maps onto (b) the low- n energy distribution which only originates from $\pi/4 < \omega t_0 < \pi/2$ in this example and spans the range W_p to $2W_p$, and (c) the high- n electron energy distribution which comes from all values of ωt_0 and spans the range W_p to $3W_p$.

we consider the geometry of the fringing fields at the hole in the top of the cavity, it is apparent that $-\nabla E^2$ is only vertical along the vertical line through the center of the hole. Thus only those electrons which pass through the center of the hole are accelerated vertically toward the detector. Most of the electrons pass through the hole off center, are accelerated at an angle from the vertical, and do not reach the detector. We estimate that $< 10\%$ of the low-energy electrons reach the detector. For electrons which have significant translational energy in the microwave field, the transverse acceleration by the fringing fields has a less pronounced effect. In other words, the hole acts as a highly achromatic diverging lens producing an overall transmission which increases smoothly with electron energy. Thus the high-energy 40s peak is much less diminished. For the 15s state, the overall size of the signal is diminished, and the sharpness of the low-energy edge is diminished.

It is straightforward to extract from data such as those of Fig. 2 the energies of the low-energy edge of the 15s and the high-energy edge of the 40s electron energy distributions. In Fig. 4 these edge energies are plotted as functions of microwave intensity. They exhibit linear dependences of $1.03(5)W_p$ and $3.45(7)W_p$, close to the

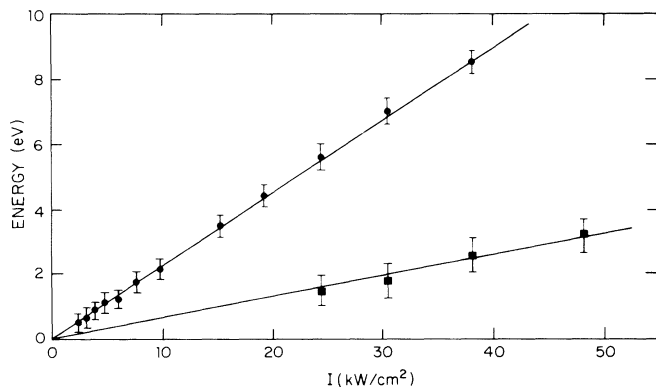


FIG. 4. Plot of the observed high-energy edge of the 40s (●) electron energy distributions, the low-energy edge of the 15s distributions (■), and linear fits (—) to the data as a function of microwave intensity. The uncertainties shown are the measurement uncertainties and do not include the microwave power uncertainty.

predicted dependences of W_p and $3W_p$, respectively, and just within the 15% microwave power calibration uncertainty.

In spite of the fact that the microwave frequency and intensity used here are, respectively 3×10^4 and 10^9 times smaller than used previously, ATI occurs and can be described in basically the same way. One major difference is that the large number of photons absorbed necessitates a classical treatment which makes particularly obvious the connection between ATI and the ponderomotive potential. A second interesting aspect is the observability of the microwave phase which we plan to observe explicitly by a more refined experiment.

It is a pleasure to acknowledge helpful conversations

with D. S. Thomson, D. J. Larson, L. A. Bloomfield, A. L'Huillier, H. B. van Linden van den Heuvell, P. Pilet, and W. Sandner. This work has been supported by the Air Force Office of Scientific Research under Grant No. AFOSR-87-0007B.

¹P. Agostini, F. Fabre, G. Mainfray, G. Petite, and N. K. Rahman, *Phys. Rev. Lett.* **42**, 1127 (1979).

²P. Krut, J. Kimman, H. G. Muller, and M. J. van der Wiel, *Phys. Rev. A* **28** 248 (1983).

³H. G. Muller, A. Tip, and M. J. van der Wiel, *J. Phys. B* **16**, L679 (1983).

⁴P. H. Bucksbaum, M. Bashkansky, and T. J. McIlrath, *Phys. Rev. Lett.* **58**, 349 (1987).

⁵L. V. Keldysh, *Zh. Eksp. Teor. Fiz.* **47**, 1945 (1965) [*Sov. Phys. JETP* **20**, 1307 (1965)].

⁶H. R. Reiss, *Phys. Rev. A* **1**, 803 (1970).

⁷H. B. van Linden van den Heuvell and T. F. Gallagher, *Phys. Rev. A* **32**, 1495 (1985).

⁸R. R. Freeman, P. H. Bucksbaum, H. Milchberg, S. Darack, D. Schumacher, and M. E. Geusic, *Phys. Rev. Lett.* **59**, 1092 (1987).

⁹H. B. van Linden van den Heuvell, R. Kachru, N. H. Tran, and T. F. Gallagher, *Phys. Rev. Lett.* **53**, 1901 (1984).

¹⁰H. B. van Linden van den Heuvell and H. G. Muller, in *Multiphoton Processes*, edited by S. J. Smith and P. L. Knight (Cambridge Univ. Press, Cambridge, 1988).

¹¹N. M. Kroll and K. W. Watson, *Phys. Rev. A* **8**, 804 (1973).

¹²H. S. Antunes Neto and L. Davidovitch, *Phys. Rev. Lett.* **53**, 2238 (1984).

¹³R. R. Freeman, T. J. McIlrath, P. H. Bucksbaum, and M. Bashkansky, *Phys. Rev. Lett.* **57**, 3156 (1986).